Acta Polytechnica CTU Proceedings **50**:1–6, 2024
https://doi.org/10.14311/APP.2024.50.0001

Published by the Czech Technical University in Prague

MODULUS ESTIMATION OF POLYMERS VIA NANOINDENTATION – IMPACT OF SURFACE ROUGHNESS, PEAK FORCE AND TESTING SPEED

Michael Huszar[a,*], Gernot Oreski[b], Florian Arbeiter[a]

[a] *Montanuniversität Leoben, Chair of Materials Science and Testing of Polymers, Otto-Glöckel-Straße 2, 8700 Leoben, Austria*

[b] *Polymer Competence Center Leoben, Sauraugasse 1, 8700 Leoben, Austria*

[*] corresponding author: michael.huszar@unileoben.ac.at

Abstract. Nanoindentation is widely used to study small-scale structures in materials. The impact of varying testing conditions on the measurement's accuracy is of high interest, and their influence on the characterization of polymeric materials is still quite scarce. Therefore, this study investigates varying loading and unloading rates paired with maximum loads ranging from 0.5 to 20 mN on Polyethylene samples with varying surface finishes after wet grinding. The indentation Data was analyzed using the Oliver & Pharr Method, and the resulting Modulus was compared with those obtained from macroscopical tensile tests. The hardness was compared to Shore hardness measurements. A correlation between the measured modulus values and the surface Quality was explored. The results prove the already established rule that the best surface finish ($S_a = 0.07\,\mu m$) leads to the smallest standard deviation. However, they show that the modulus characterization is less influenced by surface roughness than hardness evaluations.

Keywords: Polymer, nanoindentation, roughness.

1. Introduction

Nanoindentation did prove itself a valuable measuring technique for the characterization of localized mechanical properties on a micro-scale [1]. Recently, it has started to become more interesting for the field of non-linear elastic, or even visco-elastic materials [2]. One of this fields is polymer science, where foils or products with many different layers are often used. So far, these materials are most often only tested on a macroscopical scale as a whole and only limited attention is paid to the exact mechanical properties at the interfaces [3]. To successfully apply nanoindentation to polymers, several adaptations had to be introduced [4–7]. The time-dependent behavior of the materials has proven especially difficult in the past. Nevertheless, adhering to established testing routines, it is possible to accurately describe the mechanical properties of polymers on a small scale, e.g. mechanical properties resulting from small changes of local morphological properties, curing state of elastomers, or localized, time dependent behavior [8–12]. Recent studies have demonstrated the potential of nanoindentation to be used to characterize aging of polymers, which is a highly localized phenomenon [13, 14].

However, to explore localized processes while ensuring the reliability of the data obtained, it is essential to minimize possible sources of errors. Previous research on hard materials shows that the surface quality of the examined samples greatly influences results of nanoindentation [15, 16]. However, these studies focus on the hardness of metals, which exhibit different mechanical behavior compared to softer materials, such as polymers. Therefore, the influence of roughness on nanoindentation of visco-elastic materials remains a question to be addressed. The most commonly used method to characterize the surface quality from an engineering perspective is its roughness. This study uses the roughness parameter S_a to describe the different surface finishes. The focus is put on the influence of S_a on the resulting quality of nanoindentation curves and evaluated values (modulus and hardness) of a visco-elastic material. Due to the viscous nature of the tested materials, the applied maximum force and loading rate were varied to check the impact on the quality of the results as well.

2. Materials and methods

2.1. Material and sample preparation

A high-density polyethylene (PE) plate, as is often used in different polymer industries, was used in this study. Samples were cut out from this plate and wet-ground on a Struers Labopol-30 with a Laboforce-100 specimen mover (Struers, Denmark). 600, 1200, 2500, and 4000 sandpaper grits with water as lubricant and cooling agent were used for the grinding steps. One sample was polished with 3 µm diamond paste (DiaMaxx Poly, 3 µm, Akasel, Denmark) together with a lubricant for soft materials (Aka-Lube Red, Akasel, Denmark). And end-polishing was done with a fumed Silica OP-S solution (fumed silica suspension 0.2 µm water free, Akasel, Denmark) and water.

Sample finish	R_a [µm]	R_z [µm]	S_a [µm]	S_z [µm]	S_{tr}	S_{pc} [l mm^{-1}]
Sandpaper 600	1.51	14.7	1.62	25.4	0.15	3 969.49
Sandpaper 2500	0.70	7.0	0.72	13.19	0.63	2 390.63
Sandpaper 4000	0.08	1.0	0.08	2.93	0.06	1590.87
OP-S	0.05	0.8	0.07	8.3	0.31	92.89

Table 1. Results of the roughness measurements via confocal laser microscope.

To obtain parallel surfaces necessary for the indentation tests, a custom-made sample holder was used. The samples were glued to the holder with a commercially available ethyl-cyanoacrylate superglue (UHU GmbH & Co. KG, Germany, Sekundenkleber, flüssig).

Nanoindentation measurements were performed on samples with last steps of 600, 2500, 4000, and end-polished finish. The surface roughness was measured on an area of 0.9 mm^2 using a confocal laser scanning microscope VHK-1000 (Keyence, Belgium). To describe the height differences of the surface S_a (arithmetic mean) and S_z (maximum height) are used. For surface morphology, S_{tr} (texture aspect ratio) is used to characterize isotropy, and S_{pc} (arithmetic mean peak curvature) is determined to distinguish the "sharpness" of peaks. A surface with uniform roughness in all directions will have a S_{tr} near 1, while a surface with directional roughness will result in a value near 0. Sharp peaks will result in a high S_{pc} value, while a low value means more rounded, flat peaks. Additionally, within this area 10 profile lines were measured for easy comparison with the commonly used roughness values R_a and R_z.

2.2. Nanoindentation and evaluation following the Oliver Pharr approach

The nanoindentation measurements were performed on a UNHT^3 Nanoindenter (Anton Paar, Graz Austria). Subsequent evaluation was done with the software Indentation Ver.: 8.0.24 (Anton Paar, Graz Austria). A Berkovich indenter was used for all experiments. The maximum loads (F_{max}) that were used during indentations were 0.5, 1, 5, 10, 15 and 20 mN. For each load level, five indentations were made. To avoid possible interactions between indentation sites, a distance of 250 µm was used.

The indentation was performed with a loading speed of 2 times F_{max} per minute, a holding period of 10 s at F_{max} and subsequent unloading with the same speed as the loading step. The holding period is introduced to decrease the influence of visco-elastic creep on the results [17]. The unloading curve was fitted between 98 % and 40 % of F_{max} to determine the modulus. The upper and lower bounds were empirically determined in order for the tangent to describe the actual unloading curve best. The evaluation subsequently followed the method devised by Oliver and Pharr [1]. The obtained reduced modulus (E_r) is proportional to the Young´s modulus (E) of the indenter (E_{ind}) and of the sample material (in our case E_{PE}). The indenter properties are the modulus and Poisson´s ratio of diamond (E_{ind} = 1 141 GPa; ν_{ind} = 0.07), and for the Poisson´s ratio of PE, ν_{PE} = 0.4 [18] was used.

Hardness (H) is calculated using the projected area of the indenter at the contact indentation depth divided by the maximum load F_{max} [1]. Since the hardness of polymers is typically measured using a Shore durometer [19], a direct comparison of the obtained values is not possible. To achieve at least some level of comparability, the spring constant of the durometer used (Zwick, Germany) was measured, and an area function of the indenter was determined. The standard Shore D indenter features a cone-shaped tip with a 30° opening angle, and a tip radius of 0.1 mm, mounted on a cylinder with a diameter of 1.25 mm. Shore hardness is defined in a way that 100 Shore D corresponds to no penetration and 0 Shore D corresponds to no resistance, meaning the full 2.5 mm length of the indenter is pressed into the sample. Using this, the indentation depth can be calculated, and the measured spring constant of 16.77 N mm^{-1} allows the evaluation of the load at this depth to be used to calculate the hardness following [1].

3. Results and discussion

The results from the roughness measurements are shown in Table 1. For comparison, typical evaluations via line scans (R_a and R_z) and area scans (S_a, S_z, S_{tr} and S_{pc}) were used. S_a and S_z can be compared to indentation depth. Since S_z is the maximum height difference of the complete measured surface, which is much larger than the actual indentation site, it is more likely to have a height difference close to the value of S_a at the indentation area. Therefore, comparisons focus on S_a in all further analysis.

The scratches caused by the grinding of the samples led to an anisotropic surface structure. This anisotropy is especially distinct for the sample finished with the sandpaper 4000. As can be seen in Table 1, the sample shows a value of S_a = 0.08 µm while S_{tr} is close to zero (0.06).

Keeping the same indentation time settings is crucial for comparable results with different maximum loads on viscoelastic materials and their time-dependent material response. This results in different loading and unloading speeds relative to the maximum load used. In our case, speeds were set at $2F_{max}$ min^{-1}. Figure 1 shows four indentation curves

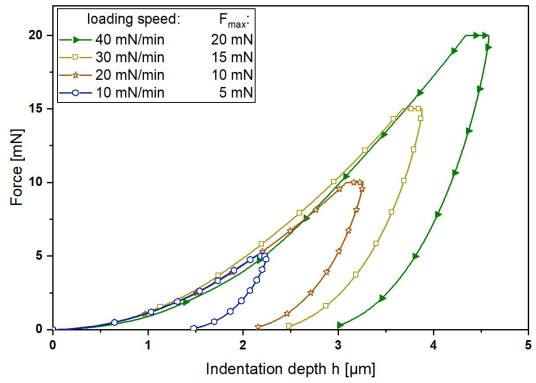

(A). Indentation curves with different F_{max} and loading and unloading speeds.

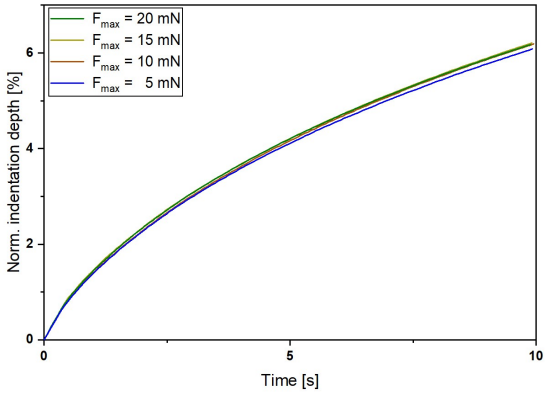

(B). The corresponding creep curves from the holding period at F_{max}.

FIGURE 1. Comparison of material response due to different F_{max} and loading and unloading speeds of $2F_{max}\,\mathrm{min}^{-1}$ on the $S_a = 0.07\,\mu\mathrm{m}$ sample.

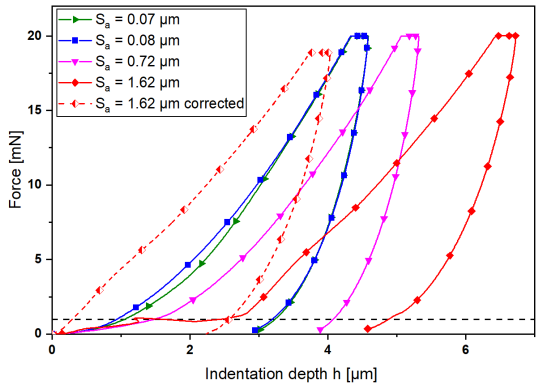

(A). Maximum load of 20 mN.

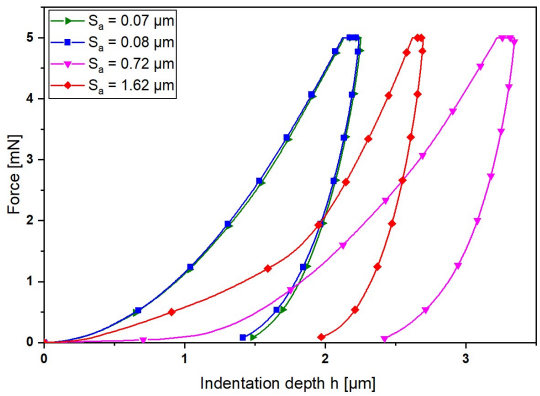

(B). Maximum load of 5 mN.

FIGURE 2. Indentation curves on the different surface finishes.

of the $S_a = 0.07\,\mu\mathrm{m}$ sample with different maximum loads, loading/unloading speeds, and a small "creep" analysis via a 10 s holding time.

As shown in Figure 1a, the loading curves of all loading speeds are almost identical. Figure 1b shows the normalized indentation depth as a function of time for all applied load levels. Similarly, there is no evident difference between the curves. While a holding segment of 10 s is insufficient for a full creep analysis, it can be used to see large deviations in the deformation and showcase different responses to the previous loading speed. These curves indicate that there is no substantial difference in the time depending material response, and therefore, the evaluations are comparable. Furthermore, the absence of a "nose" (increase of deformation depth during unloading due to viscous material effects [20]) implies that the 10 s holding time is sufficient for a precise analysis of PE samples.

After addressing the effects of loading level and speeds, the impact of surface quality was examined. Figure 2 shows a representative indentation curve of the 20 mN and 5 mN F_{max} indentations for each surface quality.

These indentation curves show that the slope of the load and unload process is strongly affected by the surface roughness. This is especially visible for the sample with the highest surface roughness of $S_a = 1.62\,\mu\mathrm{m}$. Only one successful indentation with F_{max} of 20 mN maximum load was possible for this sample. Furthermore, it shows an unconventional loading segment. The indentation curve features a long plateau, and no rising load is detected. This can indicate a badly fixed sample or indenter, and the contact point must be manually adjusted. This was done by setting the contact point after establishing a clear contact and a visible, stable growth of the indentation depth in the measured curve. This curve was evaluated for E and H before and after manually setting the contact point to compare to the other results.

Besides this faulty measurement, the influence of roughness can be seen clearly in the result from the same surface with $F_{max} = 5\,\mathrm{mN}$ (Figure 2b). There are two different slopes visible in the loading regime. The region of the first slope can be affiliated with the bending and slipping of the top of the rough surface when it comes into contact with the indenter, while the later slope starts when there is more contact with the bulk material. The same behavior can also be noticed with the $S_a = 0{,}72\,\mu\mathrm{m}$ surface indentation curves. Evaluation of these curves leads to "wrong" indentation depths, resulting in high standard deviations for the calculated E and H values, as shown in Figure 3. In contrast, there is a nearly perfect over-

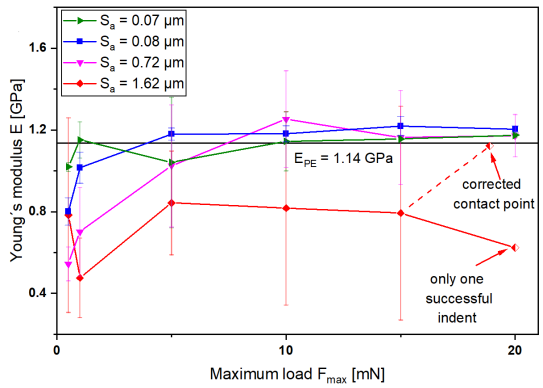

(A). The calculated values of E_{PE} compared to the Young's modulus from tensile tests.

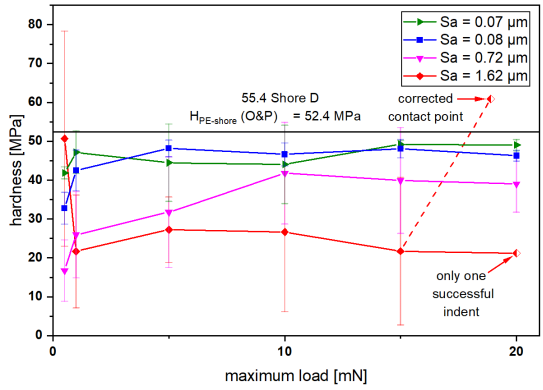

(B). H compared to a converted shore hardness result.

FIGURE 3. Dependency of indentation results on F_{max} and S_a.

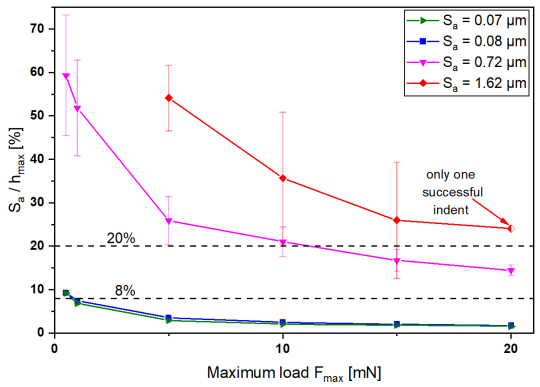

FIGURE 4. The ratio of S_a to the measured maximum indentation depth for the different surface finishes and maximum loads.

lapping of the two curves of the smooth surfaces using the 20 mN maximum load and very low deviation at the 5 mN maximum load. Based on all performed measurements, the calculated values of E and H are compared in Figure 3.

For comparison of the results, the Young´s modulus of 1.14 GPa, measured in uniaxial tensile tests in a previous research [18] and the shore hardness measured following ISO 48-4 resulting in 55.4 Shore D are used. The Shore D result was converted, following the procedure explained in section 2.2 to $H_{PE-Shore}$ = 49 MPa.

The results for Hardness and Young´s modulus follow the same trend with the two smooth surfaces, S_a = 0.07 µm (E_{PE} = 1.17 GPa; H_{PE} = 49 MPa) and S_a = 0.08 µm (E_{PE} = 1.20 GPa; H_{PE} = 46 MPa), having the lowest standard deviation and the best agreement with the macroscopic measured values. Only at the lowest value of F_{max} = 0.5 mN slight differences are detectable between these surface qualities. This deviation can most likely be attributed to the differences in S_{pc}, and the smoother peaks of the polished surface. This explains why the S_a = 0.08 µm surface is measured more compliant with the small maximum load. The S_a = 0.72 surface finish shows only good agreement for E_{PE} at a maximum load of > 10 mN, with a generally lower H_{PE} of around 40 MPa. The roughest surface in this study (S_a = 1.62 µm) shows overall lower values for E_{PE} and H_{PE} with a high standard deviation. Only the corrected contact point at F_{max} = 20 mN, resulting in E_{PE} = 1.12 GPa and H_{PE} = 61 MPa, would fit the known properties, but the chosen contact point can strongly influence the results. A not fully developed indentation due to the high surface roughness can explain these results (compare Figure 2 for F_{max} = 5 mN, where maximum indentation depth (h_{max}) is already around 25 % of S_a). They indicate that H seems more sensitive to effects caused by roughness than E. Therefore, the evaluation of H can be used more profoundly to determine if the results for the indent are correct. Overall, surface roughness strongly affects the standard deviation of both hardness and modulus characterization, with the biggest deviation on the roughest surface. To give further insights into the exact dependency of the evaluated values on the surface quality and applied F_{max} (and subsequent h_{max}), the ratios of S_a to h_{max} were assessed for all samples. Figure 4 shows the results for a quantitative comparison.

Based on the E_{PE} results presented in Figure 3 and the measurements that yielded acceptable outcomes, we can consider the ratio of approximately 20 %, achieved at a F_{max} of 10 mN for the surface with S_a = 0.72 µm as a rough threshold value for characterizing the Young's Modulus of PE via nanoindentation. The threshold for valid results seems to be much lower for hardness measurements. The level of acceptance appears to be around 8 %, reached with S_a = 0.08 µm and 0.5 mN. Since the S_a = 0.07 µm surface shows the same S_a/h_{max} ratio, the hardness results still seem to fit quite well. This is an evident sign that S_a, compared to indentation depth, is only a rough but still valuable criterion for seeing if the surface quality is good enough for specific nanoindentation evaluations.

Figure 5 depicts three indents with a maximum load of 10 mN on the surfaces with S_a = 0.72 µm, 0.08 µm, and 0.07 µm obtained with a SEM Tescan Clara (Tescan, Czech Republic).

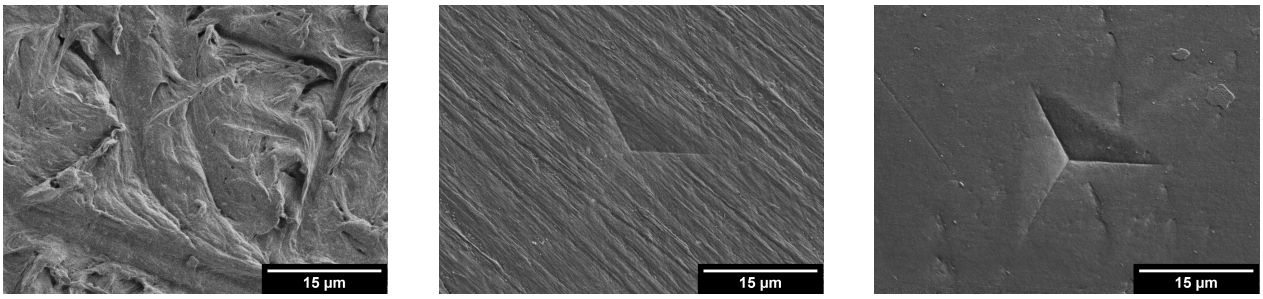

(A). $S_a = 0.72\,\mu m$. (B). $S_a = 0.08\,\mu m$. (C). $S_a = 0.07\,\mu m$.

FIGURE 5. SEM images from lasting impression of indentations with 10 mN maximum load on PE samples with different surface roughness.

While the impression can easily be seen on the best surface quality, the rougher surfaces make it hard or impossible to distinguish the indent from surface features. This can make it impossible to evaluate the correct orientation of the indenter to the surface and the tested region. The comparison between $S_a = 0.08\,\mu m$ and $S_a = 0.07\,\mu m$ shows the necessity of considering more than one roughness parameter. The lower S_{pc} of the polished surface (Figure 5c) is visible as the smoother appearance. At the same time, the difference in the S_{tr} shows the high orientation of the surface features of the $S_a = 0{,}08\,\mu m$ finish. Both differences affect the visibility of the persistent impression and the contact of the indenter to the sample material.

4. CONCLUSION

In this work, it was shown, that the applied surface preparation and subsequent roughness can significantly influence the evaluated modulus values determined via nanoindentation testing of visco-elastic materials. It has been demonstrated that with a load and unload rate below 40 mN/min, along with a 10 s holding time at maximum load, there is no significant rate-dependent effect for PE. It was possible to get reasonable results for hardness measurements with a S_a to h_{max} ratio of around 8 %, while for the modulus, a ratio of up to 20 % provided acceptable results. The results confirm that the ISO 14577 recommended R_a to indentation depth ratio of 5 % used for hardness measurements can be safely applied for polymers. Overall, it could be shown that a higher roughness increases scatter, and better statistics are required to measure the mechanical properties correctly.

ACKNOWLEDGEMENTS

The work was funded from the Polymer Competence Center Leoben GmbH and performed within the framework of the COMET-program (grant number 854178) of the Federal Ministry for Climate Action, Environment, Energy, Mobility, Innovation and Technology and the Federal Ministry for Digital and Economic Affairs, Austria.

The help from the Chair of Functional Materials and Materials Systems, in regard to roughness testing on their confocal laser scanning microscope is highly appreciated.

Grammarly was used to correct grammar mistakes and highlight complex sentences, improving the work's readability.

REFERENCES

[1] W. C. Oliver, G. M. Pharr. An improved technique for determining hardness and elastic modulus using load and displacement sensing indentation experiments. *Journal of Materials Research* **7**(6):1564–1583, 1992. https://doi.org/10.1557/JMR.1992.1564

[2] W. Gindl, H. S. Gupta. Cell-wall hardness and Young's modulus of melamine-modified spruce wood by nano-indentation. *Composites Part A: Applied Science and Manufacturing* **33**(8):1141–1145, 2002. https://doi.org/10.1016/S1359-835X(02)00080-5

[3] G. Oreski, B. Ottersböck, C. Barretta, et al. Degradation of PET – quantitative estimation of changes in molar mass using mechanical and thermal characterization methods. *Polymer Testing* **125**:108130, 2023. https://doi.org/10.1016/j.polymertesting.2023.108130

[4] P. Christoefl, J. E. Jakes, J. Geier, et al. Improved nanoindentation methods for polymer based multilayer film cross-sections. In *2023 24th International Conference on Thermal, Mechanical and Multi-Physics Simulation and Experiments in Microelectronics and Microsystems (EuroSimE)*, pp. 1–8. 2023. https://doi.org/10.1109/EuroSimE56861.2023.10100815

[5] U. D. Cakmak, T. Schöberl, Z. Major. Nanoindentation of polymers. *Meccanica* **47**(3):707–718, 2012. https://doi.org/10.1007/s11012-011-9481-6

[6] S. Yang, Y.-W. Zhang, K. Zeng. Analysis of nanoindentation creep for polymeric materials. *Journal of Applied Physics* **95**(7):3655–3666, 2004. https://doi.org/10.1063/1.1651341

[7] S. E. Arevalo, D. M. Ebenstein, L. A. Pruitt. A methodological framework for nanomechanical characterization of soft biomaterials and polymers. *Journal of the Mechanical Behavior of Biomedical Materials* **134**:105384, 2022. https://doi.org/10.1016/j.jmbbm.2022.105384

[8] P. Christöfl, C. Czibula, T. Seidlhofer, et al. Morphological characterization of semi-crystalline POM using nanoindentation. *International Journal of Polymer Analysis and Characterization* **26**(8):692–706, 2021. https://doi.org/10.1080/1023666X.2021.1968122

[9] P. Christöf, C. Czibula, M. Berer, et al. Comprehensive investigation of the viscoelastic properties of PMMA by nanoindentation. *Polymer Testing* **93**:106978, 2021. https://doi.org/10.1016/j.polymertesting.2020.106978

[10] J. Schieppati, T. Gehling, M. Azevedo, et al. Investigation into the state of cure of elastomers through nanoindentation. *Polymer Testing* **133**:108417, 2024. https://doi.org/10.1016/j.polymertesting.2024.108417

[11] A. S. Maxwell, M. A. Monclus, N. M. Jennett, G. Dean. Accelerated testing of creep in polymeric materials using nanoindentation. *Polymer Testing* **30**(4):366–371, 2011. https://doi.org/10.1016/j.polymertesting.2011.02.002

[12] M. L. Oyen. Sensitivity of polymer nanoindentation creep measurements to experimental variables. *Acta Materialia* **55**(11):3633–3639, 2007. https://doi.org/10.1016/j.actamat.2006.12.031

[13] P. Christöfl, B. Ottersböck, C. Czibula, et al. Nanoindentation for fast investigation of PET film degradation. *JOM* **74**(6):2287–2294, 2022. https://doi.org/10.1007/s11837-022-05278-0

[14] D. C. Miller, M. Owen-Bellini, P. L. Hacke. Use of indentation to study the degradation of photovoltaic backsheets. *Solar Energy Materials and Solar Cells* **201**:110082, 2019. https://doi.org/10.1016/j.solmat.2019.110082

[15] M. S. Bobji, S. K. Biswas. Estimation of hardness by nanoindentation of rough surfaces. *Journal of Materials Research* **13**(11):3227–3233, 1998. https://doi.org/10.1557/JMR.1998.0438

[16] J. Marteau, M. Bigerelle. Toward an understanding of the effect of surface roughness on instrumented indentation results. *Journal of Materials Science* **52**(12):7239–7255, 2017. https://doi.org/10.1007/s10853-017-0961-5

[17] T. Chudoba, F. Richter. Investigation of creep behaviour under load during indentation experiments and its influence on hardness and modulus results. *Surface and Coatings Technology* **148**(2-3):191–198, 2001. https://doi.org/10.1016/S0257-8972(01)01340-8

[18] M. Pletz, F. J. Arbeiter. Combined crack initiation and crack growth model for multi-layer polymer materials. *Materials* **15**(9):3273, 2022. https://doi.org/10.3390/ma15093273

[19] E. Broitman. Indentation hardness measurements at macro-, micro-, and nanoscale: A critical overview. *Tribology Letters* **65**(1):23, 2017. https://doi.org/10.1007/s11249-016-0805-5

[20] B. J. Briscoe, L. Fiori, E. Pelillo. Nano-indentation of polymeric surfaces. *Journal of Physics D: Applied Physics* **31**(19):2395, 1998. https://doi.org/10.1088/0022-3727/31/19/006